Supporting Information

Scalable Conversion of CO_2 to N-doped Carbon Foam for Efficient Oxygen Reduction Reaction and Lithium Storage

Chunxiao Xu,[a,b] *Song Chen,*[b] *Liyong Du,*[b] *Changxia Li,*[c] *Xin Gao,*[a] *Jianjun Liu,*[d] *Liangti Qu*[c] *and Pengwan Chen*[a,*]

[a] State Key Laboratory of Explosion Science and Technology, [b] School of Materials Science and Engineering and [c] School of Chemistry and Chemical Engineering, Beijing Institute of Technology, Beijing 100081, P. R. China

[d] State Key Laboratory of Chemical Resource Engineering, Beijing University of Chemical Technology, Beijing 100029, P. R. China

* Corresponding author. E-mail: pwchen@bit.edu.cn

Supporting Information Content

Pages S1 to S14

Figures S1 to S10

Tables S1 to S6

Supporting Table and Figures

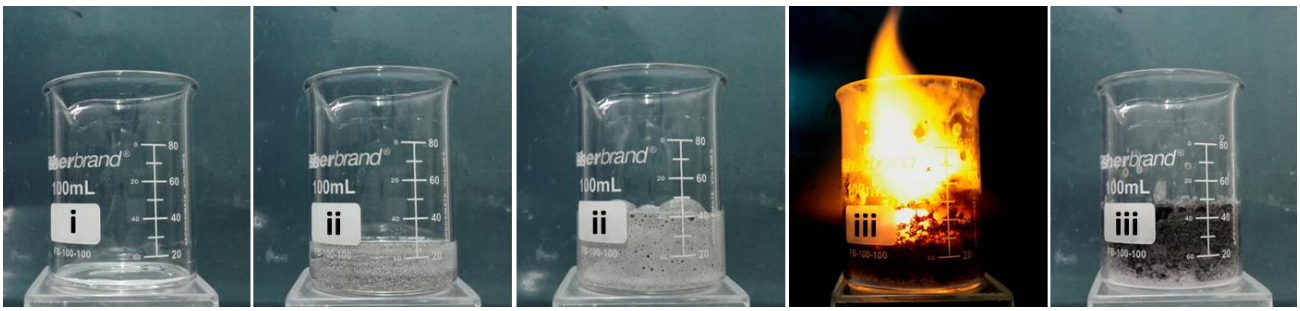

Figure S1. Experimental photographs of combustion pyrolysis conversion of CO_2 to NCF sample. (i) Chemical sorption of CO_2. (ii) Dissolution of the added Mg powders for the formation of homogeneous organic salt of magnesium. (iii) Generation of NCF under combustion pyrolysis reaction and the following acid etching treatment to remove impurities.

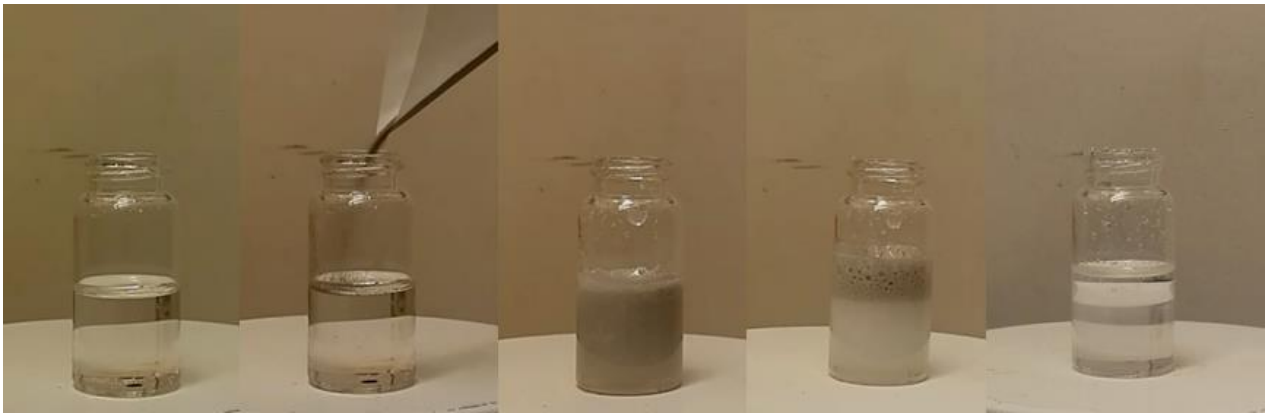

Figure S2. Experimental photographs of adding Mg powders to CO_2-saturated hydrazine hydrate solution for validation of Equation 2. The fundamental of Equation 2 is $2NH_2NH_3^+ + H_2O + Mg \rightarrow Mg^{2+} + 2NH_2NH_2 + H_2O + H_2 \uparrow$. Similiar with ammonium ion, adding water to this system could help generate more hydrogen ions through hydrolysis, thus promote the reaction of Equation 2.

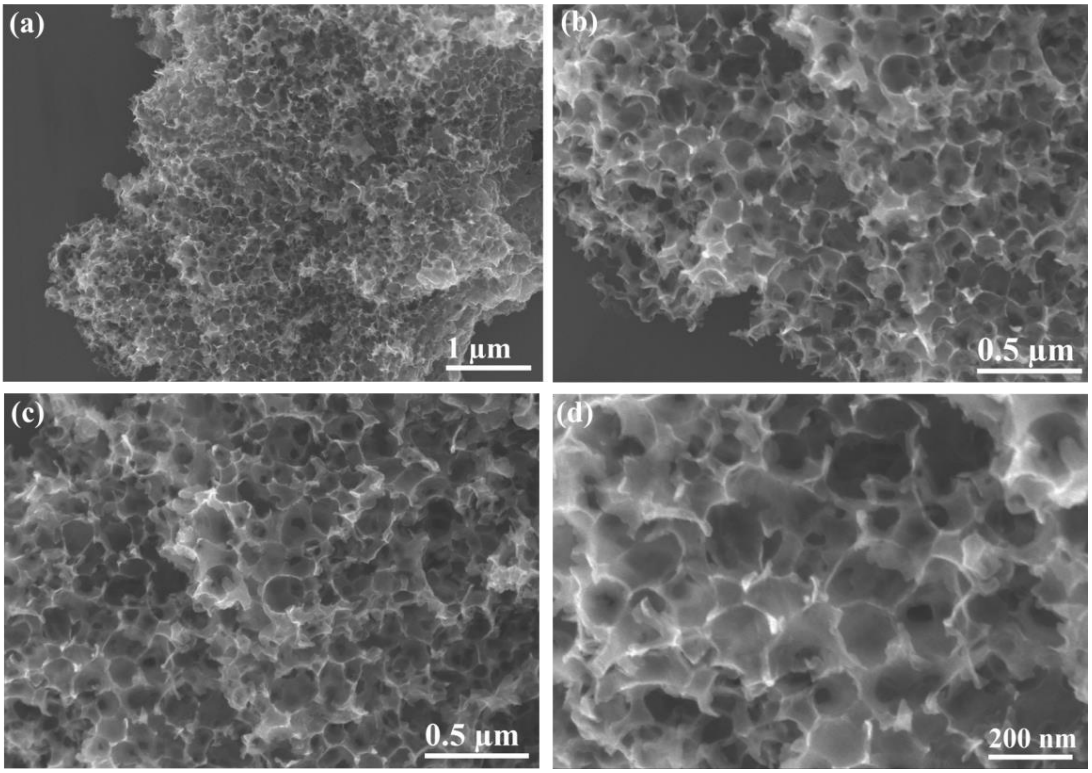

Figure S3. Low- and high-magnification SEM images of the prepared NCF_{N2H4} sample.

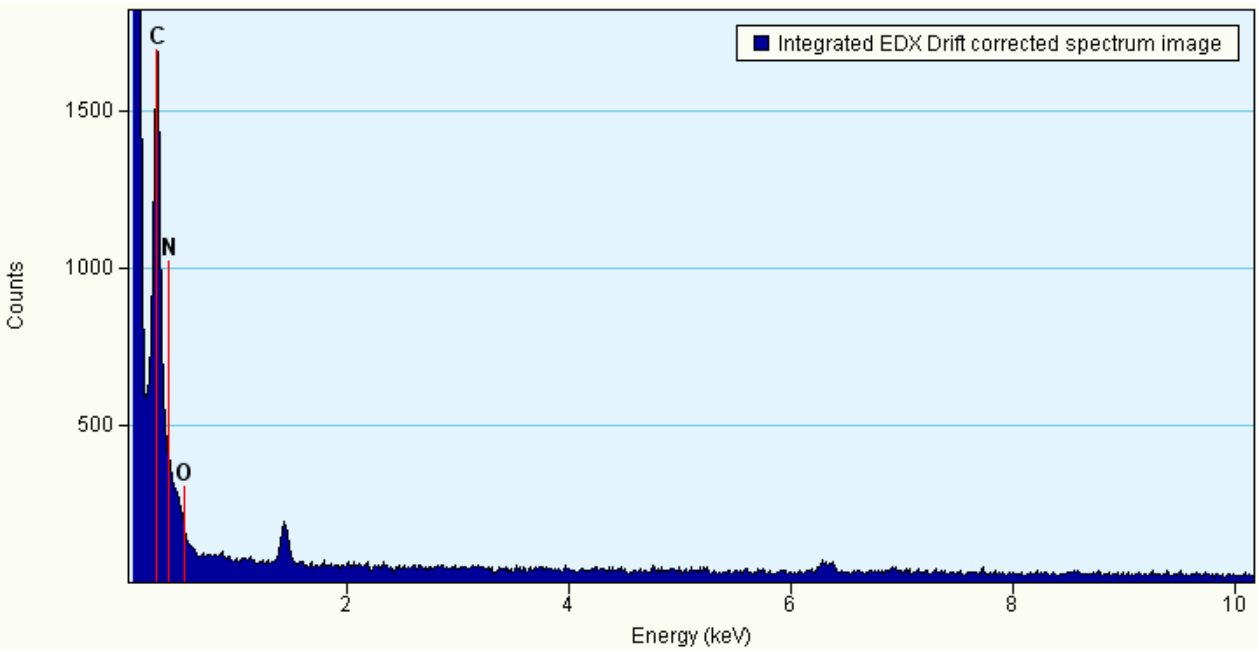

Figure S4. EDS analysis of the as-prepared NCF_{N2H4} sample.

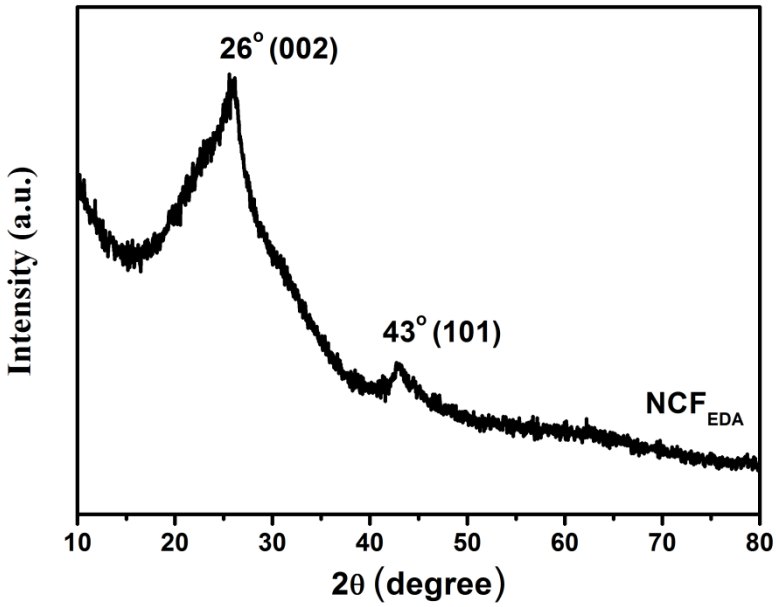

Figure S5. XRD pattern of the as-prepared NCF_{EDA} sample.

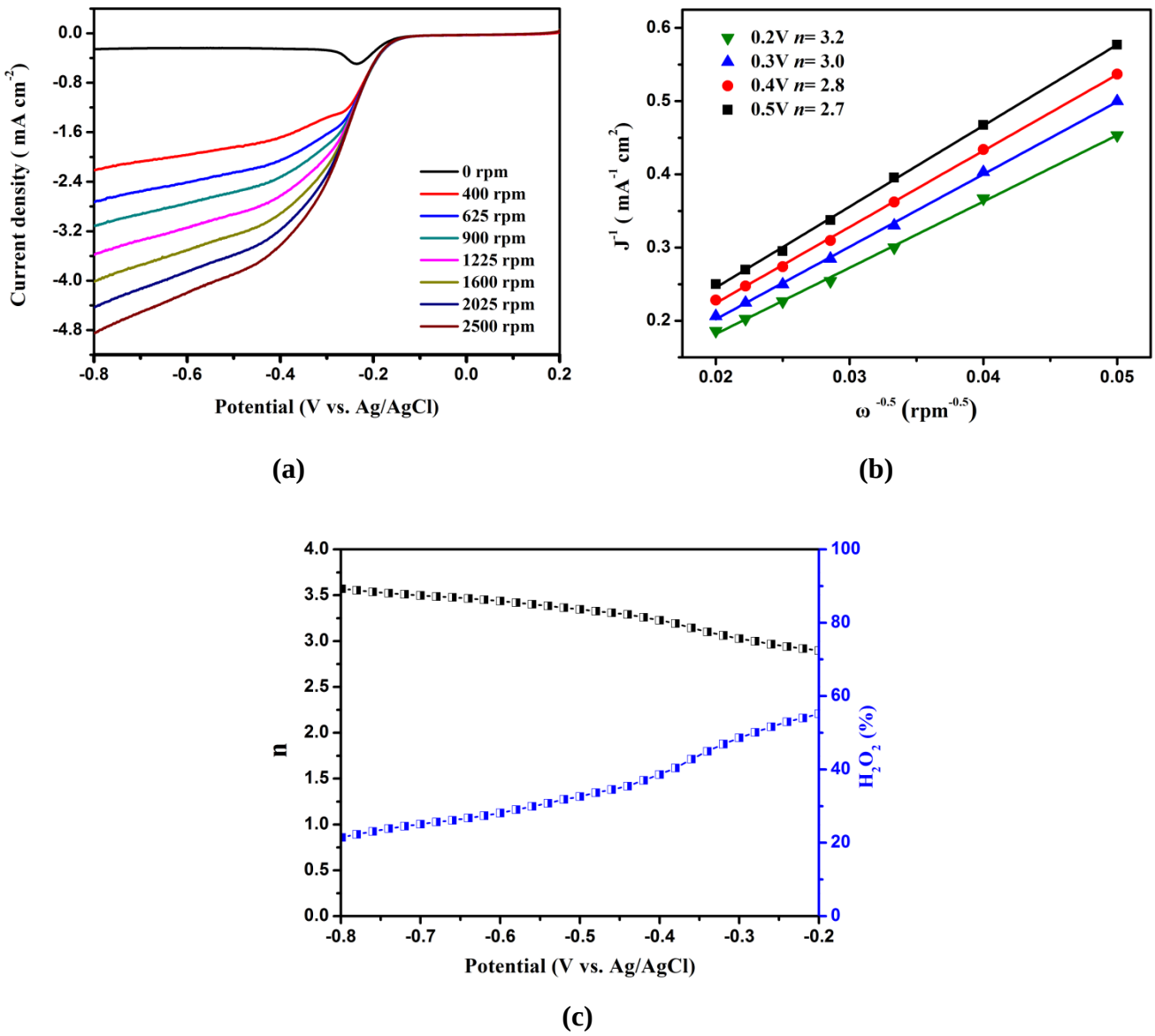

Figure S6. (a) LSV curves of NCF_{N2H4} in O_2-saturated 0.1 M KOH solution at different rotating speeds with the scan rate of 10 mV s^{-1}. (b) Koutecky–Levich plots of NCF_{N2H4} derived from LSV curves at different electrode potentials from –0.2 to –0.8 V (with mass loading of 0.16 mg cm^{-2}). (c) HO_2^- production and the corresponding *n* of the NCF_{N2H4} derived from RRED measurement.

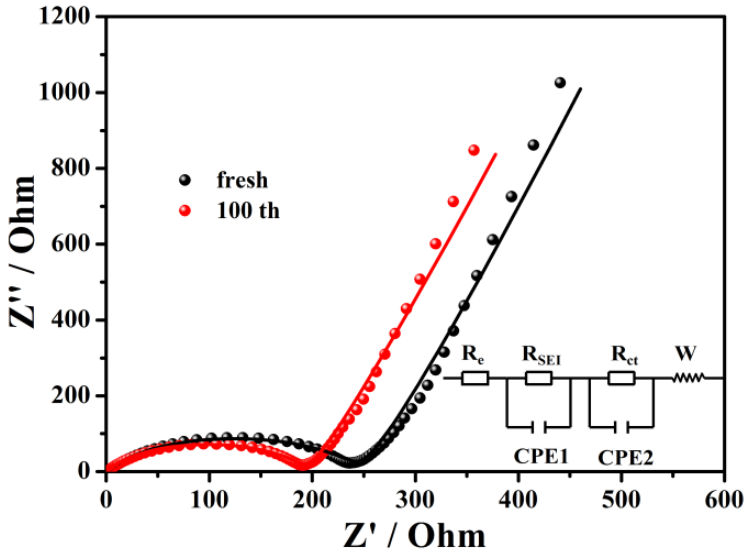

Figure S7. Nyquist plots of NCF_{N2H4} electrode before cycling and after the 100th cycles at 100 mA g^{-1}. The inset is the equivalent circuit for plot fitting.

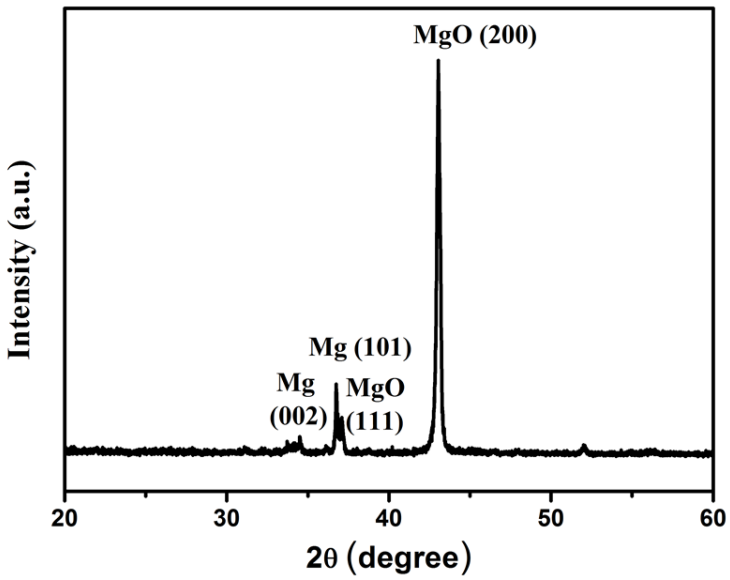

Figure S8. XRD pattern of the NCF_{N2H4} sample before acid etching.

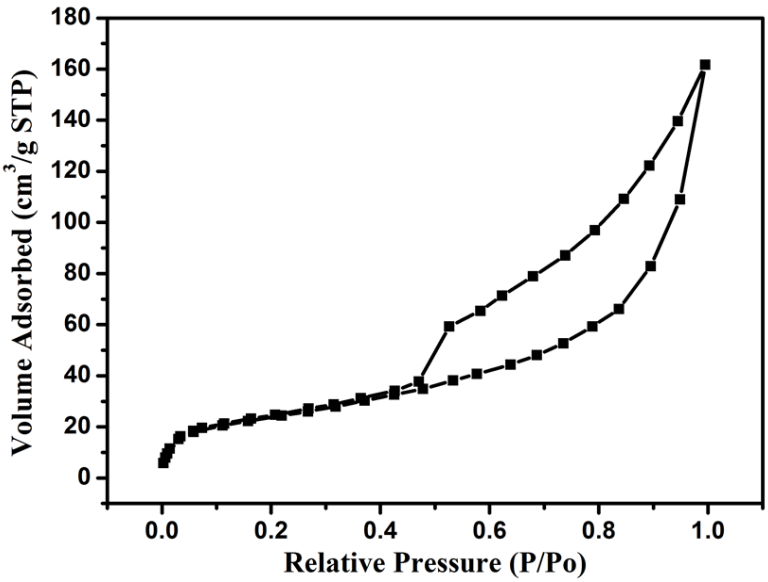

Figure S9. The nitrogen adsorption-desorption isotherm of the NCF_{N2H4} sample before acid etching. Surface Area = 85.107 m²/g, Correlation coefficient, r =0.999906.

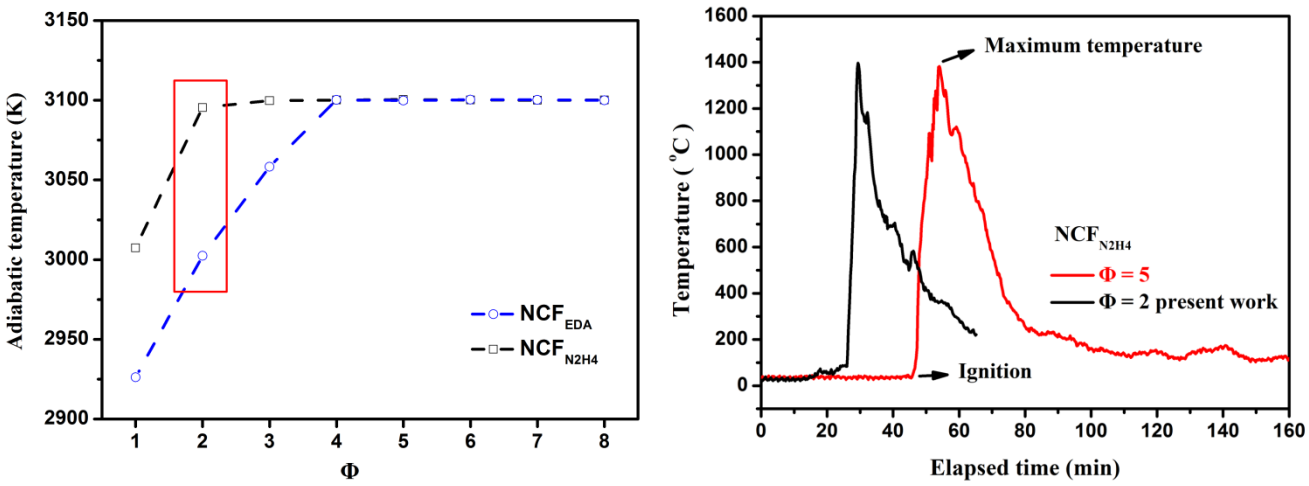

(a) **(b)**

Figure S10. (a) The calculated adiabatic temperature (Tad) of NCFs with different amount of Mg powders (ϕ from 1 to 8). (b) Measured combustion temperature−time profile of NCF_{N2H4} sample.

Table S1. Elemental analysis of NCFs based on XPS survey spectra.

Sample	C content (at.%)	O content (at.%)	N content (at.%) [a]	Pyridinic N (%) [b]	Pyrrolic N (%)	Graphitic N (%)
NCF_{N2H4}	95.37	2.51	2.12	27.08	52.04	20.88

Name	Peak BE	Height CPS	FWHM eV	Area (P) CPS.eV	Sensitivity factor RSF
C1s	284.313	132038.184	1.105	230154.9017	0.278
N1s	399.481	1745.122	4.118	8778.4500	0.477
O1s	532.167	4133.996	3.295	16995.4236	0.780

NCF_{EDA}	90.49	6.78	2.73	28.13	54.45	17.42

Name	Peak BE	Height CPS	FWHM eV	Area (P) CPS.eV	Sensitivity factor RSF
C1s	284.3	105539.16	1.142	192269.0627	0.278
N1s	399.458	1950.841	3.994	9952.7950	0.477
O1s	531.471	8911.072	4.246	40419.2587	0.780

[a] Atomic ratio $n_i/n_j = (I_i/S_i)/(I_j/S_j)$; I is calculated using the area, S is the RSF.

[b] Different kinds of chemical states are deconvoluted into corresponding peaks using XPSPEAK soft.

Table S2. Elemental analysis of NCFs based on EDS analysis.

Sample	**Element**	**Weight %**	**Atomic %**	**Uncert. %**	**Correction**	**k-Factor**
NCF_{N2H4}	C(K)	91.54	92.95	0.60	0.28	3.601
	N(K)	5.52	4.80	0.18	0.28	3.466
	O(K)	2.94	2.24	0.05	0.51	1.889
NCF_{EDA}	C(K)	90.03	91.69	0.66	0.28	3.601
	N(K)	6.31	5.51	0.35	0.28	3.466
	O(K)	3.65	2.79	0.11	0.51	1.889

Table S3. Surface area and porous size distribution of NCFs.

Sample	S_{BET} (m^2/g)	Mesopore pore size (nm)		Average pore diameter (nm)	Pore volume (cm^3/g)
NCF_{N2H4}	375.61	3.2	9.0	14.94	1.40
BET surface area: 375.6135 ± 1.9919 m²/g					
Slope: 0.011484 ± 0.000060 g/cm³ STP					
Y-intercept: 0.000103 ± 0.000011 g/cm³ STP					
C: 111.964716					
Qm: 86.2968 cm³/g STP					
Correlation coefficient: 0.9999307					
Molecular cross-sectional area: 0.1620 nm²					
NCF_{EDA}	630.81	3.2	9.0	11.71	1.85
BET Surface Area: 630.8123 ± 3.7418 m²/g					
Slope: 0.006829 ± 0.000040 g/cm³ STP					
Y-Intercept: 0.000071 ± 0.000008 g/cm³ STP					
C: 97.131388					
Qm: 144.9284 cm³/g STP					
Correlation Coefficient: 0.9999308					
Molecular Cross-Sectional Area: 0.1620 nm²					

Table S4. ORR electrocatalytic performance of synthesized NCFs and typical porous carbon-based materials in alkaline solution.

Materials	Loading (mg/cm^2)	Scan rate (mV/s)	Reduction peak (vs Ag/AgCl)	Onset potential (vs Ag/AgCl)	Reference
NCF_{N2H4}	0.16	10	–0.23 V	–0.17 V	Present work
NCF_{EDA}	0.16	10	–0.15 V	–0.09 V	Present work
N-doped Graphene Framwork	0.012	50	–0.3 V	–0.18 V	[S1]
S-Graphene Nanoplatelets	0.076	50	–0.4 V	–0.22 V	[S2]
Nitrogen-Doped Carbon Nanocages	0.08	10	–0.22 V	–0.31 V	[S3]
N-doped Ordered Macro-Mesoporous Carbon/Graphene	0.417	50	–0.28 V	–0.05 V	[S4]
Porous Carbon Nanosheets	0.11	50	–0.21 V	–0.02 V	[S5]
Mesoporous Nitrogen-Doped Carbons	0.82	50	–0.19 V	0.035 V	[S6]
Sulfur and Nitrogen -doped, Ordered Mesoporous Carbons	0.306	50	–0.16 V	–0.05 V	[S7]
N-S-doped Few Layer Graphene Oxide	0.306	50	–0.18 V	–0.11 V	[S8]
N-doped Graphene	0.04	100	–0.32 V	–0.04 V	[S9]
Nitrogen-doped Carbon Nanosheets	0.6	100	–0.28 V	–0.01 V	[S10]
N-S-doped Graphene	unknown	100	–0.24 V	–0.06 V	[S11]

Table S5. Comparison of the capacity for as-obtained NCF_{N2H4} and other typical carbon-based materials as anode electrodes in LIBs.

Materials	**Current density ($A\ g^{-1}$)**	**Specific capacity /cycling times ($mAh\ g^{-1}$)**	**Reference**
NCF_{N2H4}	0.1	881 / 100 cycles	Present work
	0.5	491	
	2	408	
	3	380	
CNT/Co_3O_4 microtubes	0.1	771 / 200 cycles	[S12]
Hierarchical NiO/Ni/Graphene hollow structure	2	962 / 1000 cycles	[S13]
SnO_2 QDs@GO	2	553	[S14]
P@CMK-3	0.2	1440/ 50 cycles	[S15]
Branched graphene nanocapsules	0.1	1454	[S16]
	0.5	1334	
	1	1175	
	2	1047	
Porous graphene networks with defects	0.37	910	[S17]
Mesoporous N-rich carbons	0.1	1780	[S18]
	0.3	865	
	1	460	
Mesoporous graphene nanosheets	0.1	770	[S19]
	0.5	430	
	2	280	
N,S co-doped porous graphene	0.1	957	[S20]
	0.5	860	
	5	560	
Carbon-nanotube/ carbon-nanofiber	0.1	1150	[S21]
	3	500	
Carbon nanorings	0.4	1237	[S22]

Table S6. Thermodynamic calculation of the adiabatic temperature of NCF_{N2H4} using "Thermo" software package.

$$4NH_2NH_2 + 2CO_2 + (\phi + 1)Mg + (\phi/2+2)O_2 \rightarrow 2C + (\phi + 1)MgO + 4N_2 + 7H_2O + H_2 \quad (S1)$$

ϕ	**Adiabatic temperature (K)**	**Gas product amount (mol)**	**Product (mol)**	
1	3007.43	13.11	H_2O (G) N_2 (G) MgO (C) C (C)	6.81 3.99 1.67 1.99
2	3095.42	13.91	H_2O (G) N_2 (G) MgO (C) C (C)	6.69 3.99 2.39 1.99
3	3099.79	14.84	Mg (G) O (G) H_2O (G) N_2 (G) MgO (C) C (C)	1.12 1.34 6.77 3.99 2.88 1.99
4	3100.15	15.77	Mg (G) O (G) H_2O (G) N_2 (G) MgO (C) C (C)	1.62 1.78 6.83 3.99 3.37 1.99
5	3100.45	16.70	Mg (G) O (G) H_2O (G) N_2 (G) MgO (C) C (C)	2.11 2.23 6.87 3.99 3.88 1.99
6	3100.13	17.64	Mg (G) O (G) H_2O (G) N_2 (G) MgO (C) C (C)	2.60 2.69 6.91 3.99 4.39 1.99
7	3100.04	18.57	Mg (G) O (G) H_2O (G) N_2 (G) MgO (C) C (C)	3.08 3.15 6.93 3.99 4.92 1.99
8	3100.14	19.51	Mg (G) O (G) H_2O (G) N_2 (G) MgO (C) C (C)	3.55 3.60 6.95 3.99 5.44 1.99

Supporting References

[S1] Zhao, Y.; Hu, C.; Hu, Y.; Cheng, H.; Shi, G.; Qu, L.; *Angew. Chem. Int. Ed.* **2012**, *51*, 11533–11537.

[S2] Jeon, I. Y.; Zhang, S.; Zhang, L.; Choi, H. J.; Seo, J. M.; Xia, Z.; Dai, L. M.; Baek, J. B. *Adv. Mater.* **2013**, *25*, 6138–6145.

[S3] Chen, S.; Bi, J.; Zhao, Y.; Yang, L.; Zhang, C.; Ma, Y.; Wu, Q.; Wang, X.; Hu, Z. *Adv. Mater.* **2012**, *24*, 5593–5597.

[S4] Liang, J.; Du, X.; Gibson, C.; Du, X. W.; Qiao, S. Z. *Adv. Mater*. **2013**, *25*, 6226–6231.

[S5] Wang, Y.; Jiang, X. *ACS Appl. Mater. Interfaces* **2013**, *5*, 11597–11602.

[S6] Yang, W.; Fellinger, T.; Antonietti, M. *J. Am. Chem. Soc.* **2010**, *133*, 206–209.

[S7] Xu, J.; Zhao, Y.; Shen, C.; Guan, L. *ACS Appl. Mater. Interfaces* **2013**, *5*, 12594–12601.

[S8] Xu, J.; Dong, G.; Jin, C.; Huang, M.; Guan, L. *Chem. Sus. Chem.* **2013**, *6*, 493–499.

[S9] Yang, S.; Zhi, L.; Tang, K.; Feng, X. L.; Maier, J.; Müllen, K. *Adv. Funct. Mater.* **2012**, *22*, 3634–3640.

[S10] Wei, W.; Liang, H.; Parvez, K.; Zhuang, X.; Feng, X.; Müllen, K. *Angew. Chem.* **2014**, *126*, 1596–1600.

[S11] Liang, J.; Jiao, Y.; Jaroniec, M.; Qiao, S. Z. *Angew. Chem. Int. Ed.* **2012**, *51*, 11496–11500.

[S12] Chen, Y. M.; Yu, L.; Lou, X. W. D. *Angew. Chem. Int. Ed.* **2016**, *55*, 5990 –5993.

[S13] Zou, F.; Chen, Y.-M.; Liu, K.; Yu, Z.; Liang, W.; Bhaway, S. M.; Gao, M.; Zhu, Y. *ACS nano* **2015**,*10*, 377-386.

[S14] Zhao, K.; Zhang, L.; Xia, R.; Dong, Y.; Xu, W.; Niu, C.; He, Li.; Yan, M.; Qu, L.; Mai, L.

small **2016**, *12*, 588–594.

[S15] Li, W.; Yang, Z.; Li, M.; Jiang, Y.; Wei, X.; Zhong, X.; Gu, L.; Yu, Y. *Nano letters* **2016**, *16*, 1546-1553.

[S16] Hu, C.; Lv, L.; Xue, J.; Ye, M.; Wang, L.; Qu, L. *Chem. Mater.* **2015**, *27*, 5253−5260.

[S17] Mukherjee, R.; Thomas, A. V.; Datta, D.; Singh, E.; Li, J. W.; Eksik, O.; Shenoy, V. B.; Koratkar, N. *Nat. Commun.* **2014**, *5*, 3710.

[S18] Li, Z.; Xu, Z.; Tan, X.; Wang, H.; Holt, C. M. B.; Stephenson, T.; Olsen, B. C.; Mitlin, D. *Energy Environ. Sci.* **2013**, *6*, 871-878.

[S19] Fang, Y. Y.; Lv, Y.; Che, R. C.; Wu, H.Y.; Zhang, X. H.; Gu, D.; Zheng, G. F.; Zhao, D.Y. *J. Am. Chem. Soc.* **2013**, *135*, 1524-1530.

[S20] Wang, Z. L.; Xu, D.; Wang, H. G.; Wu, Z.; Zhang, X. B. *ACS Nano* **2013**, *7*, 2422-2430.

[S21] Chen, Y.; Li, X.; Park, K.; Song, J.; Hong, J.; Zhou, L.; Mai, Y.W.; Huang, H.; Goodenough, J. B. *J. Am.Chem. Soc.* **2013**, *135*, 16280-16283.

[S22] Sun, J.; Liu, H.; Chen, X.; Evans, D. G.; Yang, W.; Duan, X. *Adv. Mater.* **2013**, *25*, 1125-1130.